





# Limit analysis method for active earth pressure on laggings between stabilizing piles

WANG Ming-min <sup>1</sup>  <http://orcid.org/0000-0001-8987-4203>; e-mail: 39384691@qq.com

WU Shu-guang <sup>1,2\*</sup>  <http://orcid.org/0000-0001-8138-1789>;  e-mail: wushuguang@cqu.edu.cn

WANG Gui-lin <sup>1,2</sup>  <http://orcid.org/0000-0001-5115-1165>; e-mail: glw@cqu.edu.cn

\* Corresponding author

<sup>1</sup> School of Civil Engineering, Chongqing University, Chongqing 400045, China

<sup>2</sup> Key Laboratory of New Technology for Construction of Cities in Mountain Area (Chongqing University), Ministry of Education, Chongqing 400045, China

**Citation:** Wang MM, Wu SG, Wang GL (2017) Limit analysis method for active earth pressure on laggings between stabilizing piles. Journal of Mountain Science 14(1). DOI: 10.1007/s11629-016-3935-1

© Science Press and Institute of Mountain Hazards and Environment, CAS and Springer-Verlag Berlin Heidelberg 2017

**Abstract:** Stabilizing pile is a kind of earth shoring structure frequently used in slope engineering. When the piles have cantilever segments above the ground, laggings are usually installed to avoid collapse of soil between piles. Evaluating the earth pressure acting on laggings is of great importance in design process. Since laggings are usually less stiff than piles, the lateral pressure on lagging is much closer to active earth pressure. In order to estimate the lateral earth pressure on lagging more accurately, first, a model test of cantilever stabilizing pile and lagging systems was carried out. Then, basing the experimental results, a three-dimensional sliding wedge model was established. Last, the calculation process of the total active force on lagging is presented based on the kinematic approach of limit analysis. A comparison is made between the total active force on lagging calculated by the formula presented in this study and the force on a same-size rigid retaining wall obtained from Rankine's theory. It is found that the proposed method fits well with the experimental results. Parametric studies show that the total active force on lagging increases with the growth of the lagging height and the lagging clear span; while decreases as

the soil internal friction angle and soil cohesion increase.

**Keywords:** Stabilizing pile; Lagging; Active earth pressure; Limit analysis method; Sliding surface

## Introduction

Stabilizing piles are frequently used in slope engineering. Since piles are discontinuous in horizontal direction, if they have cantilever segments above the ground, laggings are generally installed to avoid soil collapse between two adjacent piles. The lagging usually consist of rough sawn timber, concrete plank or metal decking. On the premise of ensuring safety, the thinner lagging used in construction, the more economical the engineering project could be. Hence, accurate evaluation of lateral earth pressure on lagging is of great importance in design process.

In continuous earth retention systems (e.g. rigid retaining wall), lateral earth pressure is generally assumed to be constant along the length of the wall, and the plane-strain assumption can be

**Received:** 08 March 2016  
**Revised:** 08 June 2016  
**Accepted:** 17 November 2016

used to simplify the analysis mode (Terzaghi 1943; Wang 2000; Paik and Salgado 2003). While in stabilizing pile and lagging systems, lagging is often considerably less stiff than pile. This kind of stiffness variation aims at utilizing the soil arching effects so as to transform more earth pressure on pile. However, it increases the difficulty to calculate earth pressure on lagging.

Estimating the lateral earth pressure on lagging has always been an important field of study for geotechnical engineering both in theory and practice. Since Terzaghi (1943) explained the phenomenon of pressure transfer from a yielding mass of soil to adjacent soil by the “trap-door test”, the soil arching effect became a widely accepted interpretation of the earth pressure reduction on laggings. Macnab (2002) used the portion of the active earth pressure in different distributions to estimate the reduced soil pressure on laggings. Vermeer et al. (2001) performed a study of arching effect behind a soldier pile wall and estimated the lateral earth pressure on laggings using non-linear 3D finite element method and in-situ tests. Besides the soil arching effects, Howard and John (2008) introduced a theoretical model based on the “silo” shaped sliding wedge analysis to determine the lateral earth pressures on wood laggings. Dong (2009) performed a study of three-dimensional soil arching effect of cantilever piles. Dong et al. (2009) proposed that the failure mode of the soil between cantilever piles mostly showed as sliding.

The Limit analysis method is a well-developed theory which can solve earth pressure problems (Chen 1975; Yang 2007; Shukla et al. 2009; Soubra and Macuh 2002). By idealizing the soil as a perfect plastic material obeying an associated flow rule, two plastic bounding theorems (upper and lower bounds) can be proved. Even though most of operating processes of limit analysis method are limited to two dimensions, publications about this theory using in three dimensional problems are also available (Chen et al. 2001; Michalowski and Drescher 2009; Han et al. 2014; Gao et al. 2012; Skrabl and Macuh 2005). However, those existing methods are not applicable to calculation of lateral earth pressure on lagging between stabilizing piles, due to the more complex boundary condition and the arching effect which controls the mechanical behavior of soils between piles. The main challenge in estimating the lagging earth pressure based on

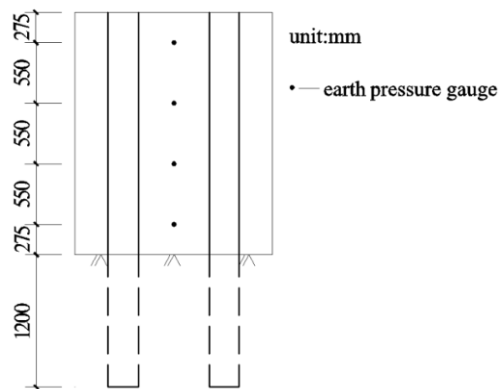
the upper bound method is to examine the three-dimensional failure mechanism.

In present work, efforts are made to develop predictive model for the total active force on laggings caused by backfills between stabilizing piles. First of all, a model test of cantilever stabilizing pile and lagging systems is carried out to research the earth pressure acting on laggings and the translational failure mechanism of the backfill between cantilever piles. Second, a three-dimensional translational failure mechanism of the soil between two piles is established. The geometry of the admissible mechanism is described analytically, and the most critical mechanism is found based on an optimization routine. The total active force on lagging based on the energy-work balance equation is compared with the experimental result to test its validity. Third, the value of total active force on lagging based on the three-dimensional upper bound method is compared with the lateral force acting on same-size rigid retaining wall based on Rankine’s theory. Finally, the effects of lagging height  $h$ , lagging clear span  $w$ , internal friction angle  $\varphi$ , and cohesion  $c$  on active earth pressure of laggings are analyzed.

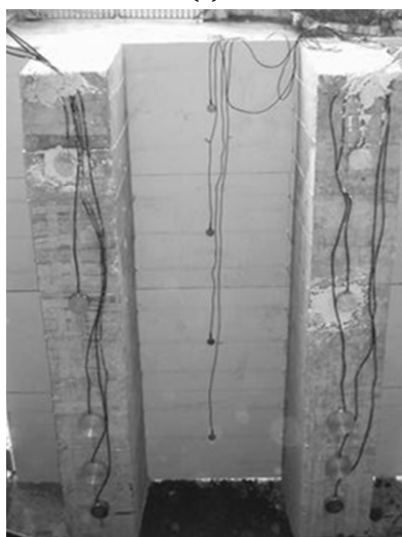
## 1 Model Test of Cantilever Stabilizing Pile and Lagging Systems

To research the translational failure mechanism of the soil between cantilever piles, in situ model test was carried out. The experiment was made on the two cantilever piles in an artificial slope site. In order to meet the requirements of small rigidity, good flexibility and homogeneous mechanical property, high density board (wood) was used to made laggings, and the thickness of board was 18mm. The flexible high density board was arranged between the piles. The top surface of the slope was horizontal; the cross section of the stabilizing piles was rectangular with length of 0.5 m and width of 0.3 m; The height of lagging was 2.2m (represented by  $h$ ), and the clear span of lagging was 0.7 m (represented by  $w$ ). Filling soil behind the piles was fine sand, the parameters of the soil were  $\varphi=28^\circ$ ,  $c=1.0\text{kPa}$  and  $\gamma=16.1\text{kN/m}^3$ . Embedded depth of piles was 1.2m, spacing of piles was 1m, and concrete with 20MPa cube compressive strength was used in pouring piles.

Five resistance-type earth pressure gauges were arranged on the span of the back of the baffle. The location of the earth pressure gauge is shown in Figure 1. The stabilizing piles were considered as rigid bodies with no displacement, and the gap between lagging and soil was filled with loose sands.



(a)



(b)

Figure 1 The location of the earth pressure gauge.

After 24 hours, earth pressure of each measuring point in the span of the baffle was measured when soil mass was stable enough behind the piles. Utilizing these data, the curve of soil pressure between piles was obtained as shown in Figure 2. Assuming that the soil pressures were equal to each other at the same level on the baffle, according to the product of the figure area of the area enclosed by soil pressure curve and coordinate axes multiply and the span of the baffle plate, the active earth pressure between piles could be evaluated and the number is 1.1 kN. After earth

pressure measurement was finished and baffle was removed, soil between the cantilever piles began to collapse. The damage situation is shown in the Figure 3.

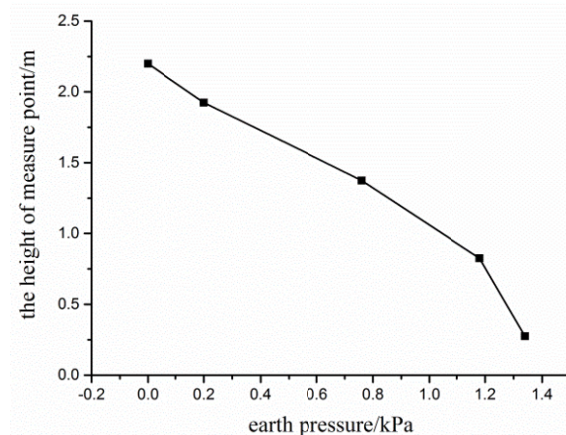


Figure 2 Testing results of earth pressure.



Figure 3 Instability phenomenon of soils between cantilever piles in tests.

## 2 Three-dimensional Translational Failure Mechanism

In order to make full use of the soil arching effects, lagging between piles is often made less stiff than pile, or the gap between lagging and soil is filled with loose sands. These allow the wedge-shaped soil mass located back of the lagging (called the *sliding wedge*) to have potential downward movement. As a result, the pressure on lagging is closer to active earth pressure.

Since the sliding wedge behind lagging is a three-dimensional entity, it cannot be simplified to a plane-strain model. In order to use the kinematic approach of limit analysis, a suitable three-

dimensional mechanism of failure must be established first.

By analyzing some experiment phenomena of soil collapse between two adjacent piles, Zhang et al. (2014) summarized the features of sliding surface between two adjacent piles as follows: (1) the sliding surface is symmetrical to a neutral plane, which is at the middle of the spacing between two piles; (2) the intersection of the sliding surface and a horizontal plane is a parabola; (3) the intersection of the sliding surface and a vertical plane (perpendicular to lagging) can be approximated as a straight line. These features fit with the experimental results of in situ model test and Zhou's (2009) numerical and analytical result also prove.

Based on these features, a three-dimensional translational failure mechanism is established as shown in Figure 4. The soils behind lagging are divided into two parts by a velocity discontinuity surface (sliding surface), which can be interpreted as limits of thin material layers undergoing shear and possibly dilation. Soils on each side of the sliding surface are considered as a rigid block. The sliding surface is generated by moving a generatrix (straight line) along a directrix (parabola). The directrix is on the top horizontal surface of backfills, and the intersection of the directrix and the lagging locates on the side surface of the pile.

Figure 5 shows the top and side views of the sliding wedge model. Line  $OG_0$  is the back of the lagging. Line  $E_0G_0$  is the generatrix on the neutral plane. The height of lagging is  $h$ ; and the clear span of lagging is  $w$ . The angle of shearing resistance of backfills is  $\varphi$ ; the cohesion of backfills is  $c$ . The unit weight of backfills is  $\gamma$ ; and the inclination angle between the generatrix and vertical is  $\beta$ .

Since it is difficult to calculate the power of gravity  $W_g$  and the rate of internal energy dissipation (represented by  $D$ ) directly, a further treatment of the sliding wedge model is presented (Figure 6). As the symmetry is considered, only half of the sliding wedge is adopted. The sliding wedge is divided into several slices by a set of planes (represented symbolically by  $K_i$ ), which parallel with the  $yo$ z plane. The number of planes is  $(n+1)$ , and the space between two adjacent planes is  $w/(2n)$ . By moving the generatrix on  $K_i$ , another plane (represented by  $J_i$ ) is generated, which parallels with the  $x$  coordinate axis. The

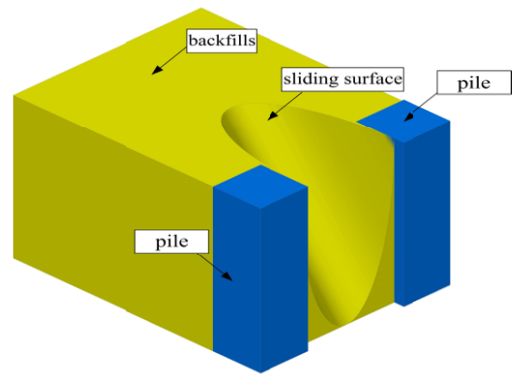


Figure 4 Three-dimensional translational failure mechanism of soil between piles.

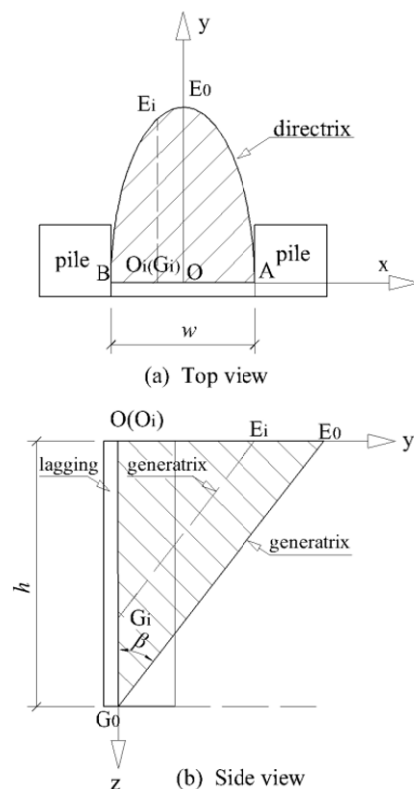


Figure 5 Top and side views of three-dimensional sliding wedge model.

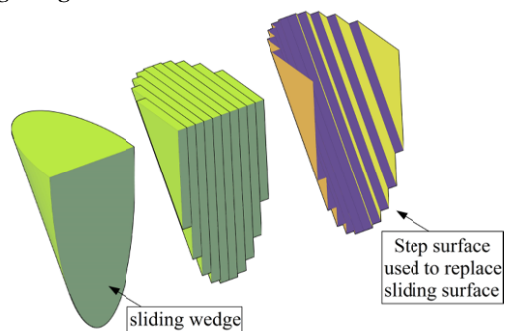


Figure 6 Simplification process of three-dimensional sliding surface.



generatrix on  $K_i$  meets the directrix at the point  $E_i$ . Then the sliding surface can be replaced by a step surface (Figure 6).

After the simplification of three-dimensional sliding surface, the equation of the directrix can be postulated as:

$$y_i = ax_i^2 + b \tag{1}$$

In Eq.(1),  $a$  and  $b$  are coefficients to be determined. Since the coordinates of point A and point B are known, it can be derived that:

$$a = -\frac{4h \tan \beta}{w^2} \tag{2}$$

$$b = h \tan \beta \tag{3}$$

In addition, the following relationships are met:

$$O_i E_i = -\frac{4h \tan \beta}{w^2} \left(i \cdot \frac{w}{2n}\right)^2 + h \tan \beta \tag{4}$$

$$E_0 G_0 = \sqrt{h^2 + (h \tan \beta)^2} \tag{5}$$

$$O E_0 = h \tan \beta \tag{6}$$

$$E_i G_i = h \left(1 - \frac{i^2}{n^2}\right) \sqrt{1 + \tan^2 \beta} \tag{7}$$

$$O_i G_i = h \left(1 - \frac{i^2}{n^2}\right) \tag{8}$$

### 3 Calculation Procedure of the Total Active Force on Lagging

It is pretty complex when considering the friction/adhesion between the soil backfill and the lagging face. In this paper, the lagging between piles is assumed smooth, and backfill behind the pile is low cohesive soil or sandy soil. Thus, in deriving the total active earth pressure on lagging (represented by  $P_a$ ), the friction/adhesion between the soil backfills and the lagging surface is neglected. Hence the earth pressure on lagging (represented by  $P$ ) is perpendicular to the lagging surface. According to the basic assumption of the upper bound theory, full shear strength of the failure plane is mobilized.

#### 3.1 Input energy and energy dissipation of the instability mechanism

Since the sliding wedge is divided into several slices by plane set  $K_i$ , the power of gravity  $W_g$  could

be obtained by summing up the power of gravity of each soil slice:

$$W_g = 2 \cdot \sum_{i=0}^{n-1} W_{g_i} = 2 \cdot \sum_{i=0}^{n-1} \left[ \frac{1}{2} O_i E_i \cdot O_i G_i \cdot \frac{w}{2n} \cdot \gamma \cdot V \cos(\varphi + \beta) \right] \tag{9}$$

The negative work done by the counterforce, from lagging to sliding wedge, is

$$W_p = -PV \sin(\beta + \varphi) \tag{10}$$

In view that the sliding surface has been replaced by a step surface (Figure 6), the rate of internal energy dissipation of the sliding surface comprises two parts: the plane set  $K_i$  (vertical plane), and the plane set  $J_i$  (inclined plane). The rate of internal energy dissipation of the plane set  $J_i$  can be calculated based on Mohr-Coulomb material. Basing on the associated flow rule, the angle between velocity  $V$  (the velocity of sliding wedge) and the plane set  $J_i$  is  $\varphi$ . And the energy dissipation rate is the product of tangential velocity ( $V \cos \varphi$ ), cohesion and the area of  $J_i$ . Thus, this part of energy dissipation rate is shown in Eq. (11).

$$D_j = 2 \cdot \sum_{i=0}^{n-1} \left( E_i G_i \cdot \frac{w}{2n} \cdot V \cos \varphi \cdot c \right) \tag{11}$$

While the material of the sliding surface  $K_i$  could not be considered as Mohr-Coulomb material (considering the bilateral symmetry, there is no dilation occurring in the plane set  $K_i$ ), the energy dissipation rate of plane set  $K_i$  should be calculated as Tresca material. The sum area of  $K_i$  is  $O E_0 G_0$ , and this part of energy dissipation rate can be presented as:

$$D_k = 2 \cdot \left( \frac{1}{2} O E_0 \cdot O G_0 \cdot V \cdot c \right) \tag{12}$$

Since the flow rule associated with Mohr-Coulomb yield condition (for soils with  $\varphi > 0$ ) predicts greater dilation than that measured in experiments, the energy dissipation rate of Mohr-Coulomb material is underestimated while the rate of Tresca material is overestimated. Hence, the accuracy of overall energy dissipation rate is increased by error compensation.

The total energy dissipation rate of the slip surface, which has been replaced by a step surface ( $J_i$  and  $K_i$ ), can be calculated by adding  $D_j$  and  $D_k$ . The total energy dissipation rate is shown in Eq. (13).

$$D = D_j + D_k = 2 \cdot \left[ \sum_{i=0}^{n-1} \left( E_i G_i \cdot \frac{w}{2n} \cdot V \cos \varphi \cdot c \right) + \frac{1}{2} O E_0 \cdot O G_0 \cdot V \cdot c \right] \tag{13}$$

After the input energy and energy dissipation of the instability mechanism have been obtained, the total active earth pressure on lagging (represented by  $P_a$ ) can be calculated by the work-energy balance equation.

### 3.2 Work-energy balance equation

By equating the power of external forces to the internal energy dissipation in the failure mechanism, Eq. (14) is obtained.

$$2 \cdot \sum_{i=0}^{n-1} \left[ \frac{1}{2} O_i E_i \cdot O_i G_i \cdot \frac{w}{2n} \gamma V \cos(\varphi + \beta) \right] - PV \sin(\beta + \varphi) = 2 \cdot \left[ \sum_{i=0}^{n-1} \left( E_i G_i \cdot \frac{w}{2n} \cdot V \cos \varphi \cdot c \right) + \frac{1}{2} O E_0 \cdot O G_0 \cdot V \cdot c \right] \quad (14)$$

Putting the geometrical relationships (4)-(8) into Eq. (14), Eq. (15) is obtained.

$$h \tan \beta \gamma w \cos(\varphi + \beta) \sum_{i=0}^{n-1} \left[ \left( 1 - \frac{i^2}{n^2} \right)^2 \frac{1}{n} \right] - P \sin(\varphi + \beta) = 2 \sqrt{1 + \tan^2 \beta} \cdot \cos \varphi \cdot c \cdot w \sum_{i=0}^{n-1} \left[ \left( 1 - \frac{i^2}{n^2} \right) \cdot \frac{1}{n} \right] + 2 \tan \beta \cdot h \cdot c \quad (15)$$

When  $n$  goes towards infinity, the following relationship holds.

$$\lim_{n \rightarrow \infty} \sum_{i=0}^{n-1} \left[ \left( 1 - \frac{i^2}{n^2} \right) \frac{1}{n} \right] = \frac{2}{3} \quad (16)$$

$$\lim_{n \rightarrow \infty} \sum_{i=0}^{n-1} \left[ \left( 1 - \frac{i^2}{n^2} \right)^2 \frac{1}{n} \right] = \frac{8}{15} \quad (17)$$

Putting Eq. (16) and (17) into Eq. (15), Eq. (18) can be obtained.

$$P = \left[ \frac{8}{15} h \tan \beta \cdot \gamma \cdot w \cos(\varphi + \beta) - \frac{4}{3} \sqrt{1 + \tan^2 \beta} \cdot \cos \varphi \cdot c \cdot w - 2 \tan \beta \cdot h \cdot c \right] / \sin(\varphi + \beta) \quad (18)$$

If the geometrical parameters of the model and the strength parameters of the soils are known, several hypothetical instability mechanisms (represented by different  $\beta$ ) and the corresponding total earth pressure on lagging (represented by  $P$ ) can be determined. By solving the derivative of  $P$ , the maximum value of  $P$  is obtained. The maximum value of  $P$  corresponds to the most unstable mechanism of soil between piles, and it is the total active earth pressure on lagging (represented by  $P_a$ ).

The maximum value of  $P$  can be determined by an optimization routine. This procedure is explicit when  $\varphi = 0$ , and implicit otherwise.

It should be mentioned that the Eq. (18) has its applicable conditions. To be more specific, the lagging between piles should be smooth and filling soil behind the pile should be low cohesive soil or sandy soil.

## 4 Application Example and Parameter Analysis

To illustrate the validity of the method mentioned above, comparing the total active earth pressure got by proposed methods with the experimental results got by model test is believable. Based on Eq. (18), the relationship between  $P$  and  $\beta$  of the example is presented in Figure 7. It can be calculated that the value of total active earth pressure on lagging,  $P_a$ , is 1.01kN. It is pretty close to the experimental results (1.1kN), which has been evaluated in chapter 2. In consideration of the measurement error and simplification error, the proposed methods can be used in evaluated the earth pressure on laggings.

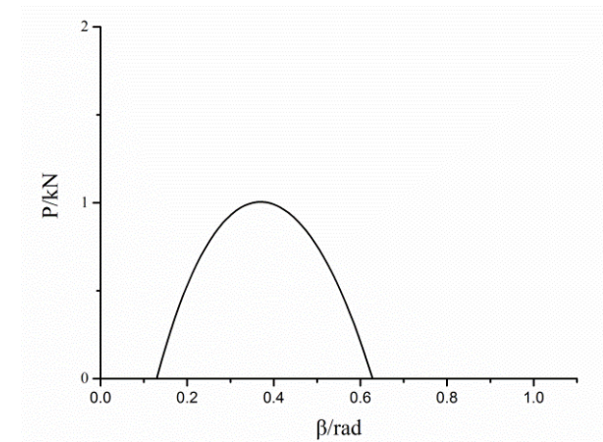


Figure 7 Relationship between  $P$  and  $\beta$  of the original example.

In order to evaluate the effects of lagging height  $h$ , lagging clear span  $w$ , soil internal friction angle  $\varphi$ , and soil cohesion  $c$  on the active earth pressure of lagging, parametric analyses are carried out.

### 4.1 Effects of lagging height $h$

To investigate the effects of lagging height  $h$  on the total active earth pressure of lagging,  $h$  is varied from 1 m to 8 m while other parameters are kept as

the constant as mentioned above.

The relationship between  $P_a$  and  $h$  is illustrated in Figure 8. It also shows the total active force acting on a rigid retaining wall with the same size of the lagging, which is calculated by Rankine's theory (1943). It is observed that the value of the active force on lagging obtained from the present analysis is smaller than the value obtained from Rankine's theory for the same set of parameters, especially at larger value of  $h$ . This is partly due to the using of the three-dimensional translational failure mechanism in which the arching effects and the constraints of adjacent soils are considered in lagging's earth pressure calculation.

Experience has shown that the soil pressure on lagging is generally constant with depth increasing. Deeper excavations typically do have a thicker lagging. So the total active force on lagging should be proportional to the lagging height  $h$ , which is confirmed in this study.

#### 4.2 Effects of lagging clear span $w$

To investigate the effects of lagging clear span  $w$  on  $P_a$ ,  $w$  is varied from 0.5 m to 5 m while maintain other parameters unchanged as the original example. The relationship between  $P_a$  and  $w$  is illustrated in Figure 9. As can be seen,  $P_a$  increases linearly with the increasing lagging clear span  $w$ .

It is also found that the total active force on lagging is less than that on retaining wall of the same size. As  $w$  increases, the ratio of active force on lagging to active force on retaining wall decreases. This fits the common practice in that the soil arching effects becomes non-significant when pile spacing increases.

#### 4.3 Effects of soil internal friction angle $\phi$

Effects of soil internal friction angle  $\phi$  on total active earth pressure of lagging corresponding to different  $c$  are shown in Figure 10. Other parameters are equal to the original example. As can be seen,  $P_a$  decreases non-linearly with the increasing internal friction angle  $\phi$ .

#### 4.4 Effects of soil cohesion $c$

Effects of soil cohesion intercept  $c$  on total active earth pressure of lagging corresponding to different  $\phi$  are shown in Figure 11. As can be seen,

$P_a$  decreases linearly with the increasing cohesion intercept  $c$ . The decrease rate of  $P_a$  becomes gentler for the larger value of internal friction angle  $\phi$ .

It was found that a small amount of cohesion significantly reduced the computed pressure on the

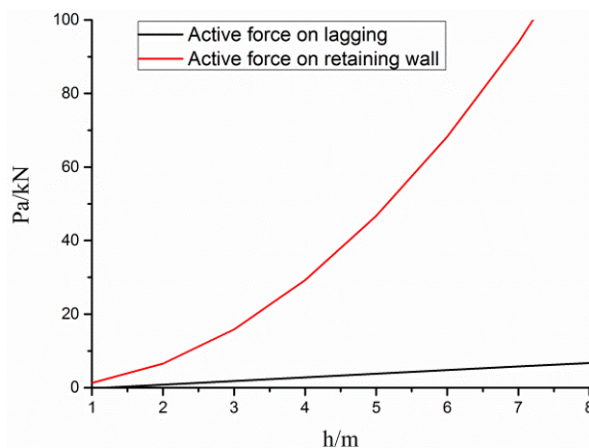


Figure 8 Relationships between  $P_a$  and  $h$ .

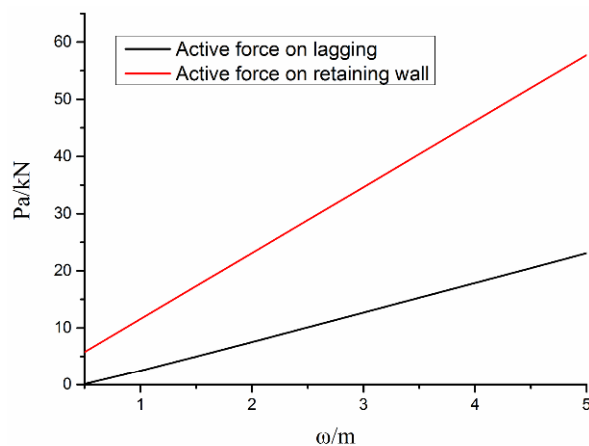


Figure 9 Relationships between  $P_a$  and  $w$ .

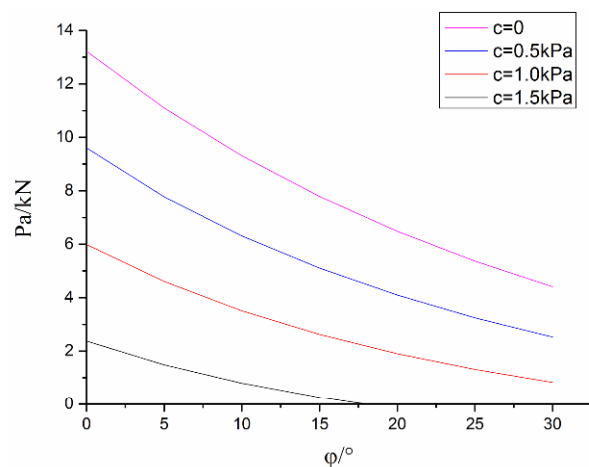
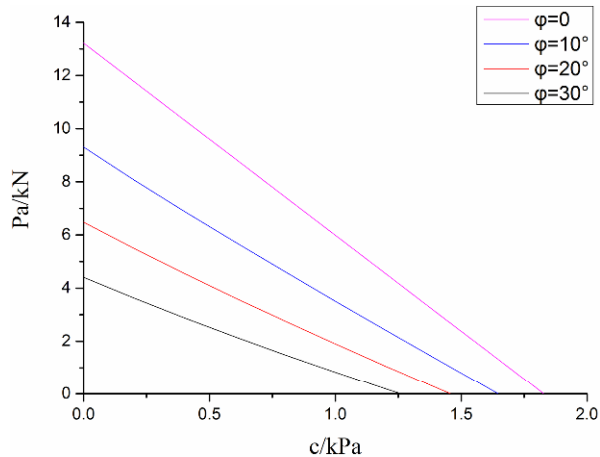


Figure 10 Relationships between  $P_a$  and  $\phi$ .

lagging. This matches the phenomenon that cohesive soil behind lagging seldom comes into contact with the lagging. The decreasing rate of  $P_a$  becomes smaller for a higher internal friction angle  $\varphi$ .



**Figure 11** Relationships between  $P_a$  and  $c$ .

If the cohesion of backfills is considered, it should be mentioned that cohesion can dissipate over time with the invasion of moisture. Hence, the use of cohesion in the design of pile and lagging systems should be carefully dealt with.

## 5 Conclusions

The general conclusions of the present study are summarized as follows:

- (1) A model test of cantilever stabilizing pile and lagging systems was carried out, in which a three dimensional sliding surface is observed.
- (2) A three-dimensional translational failure mechanism for calculating the total active earth pressure on lagging is presented, which involves the soil arching effects implicitly;
- (3) The calculation procedure of total active

force on lagging is presented based on the kinematic approach of limit analysis;

(4) The results based on the proposed method are compared with those obtained from Rankine's theory based on plane-strain assumption, and the new method is proved to fit well with the experimental result;

(5) The total active force on lagging increases with the lagging height  $h$  linearly, matching the experience that the soil pressure on lagging is generally constant with depth increasing;

(6) The total active force on lagging increases with the growth of lagging clear span  $w$ . As  $w$  increases, the ratio of active force on lagging to active force on retaining wall decreases, indicating that the soil arching effect is less obvious for the large space of piles;

(7) The total active force on lagging decreases non-linearly with the increase of soil internal friction angle  $\varphi$ , and decreases linearly with the increase of soil cohesion  $c$ .

It should be noted that the total active force obtained from this study is only suitable for a specified three-dimensional failure mechanism which involves the soil arching effects implicitly. That is to say, the pile spacing should be satisfied with the condition of arch forming. If the backfills of a soldier pile and lagging system is soft clay or below the groundwater table, where there is no arching effect in the soils between piles by experience, the lateral force acting on lagging may be greater than the predicted value.

## Acknowledgments

The research work is financially supported by the National Key Technology Research and Development Program of the Ministry of Science and Technology of China under Grant No. 2012BAJ22B06.

## References

- Chen WF (1975) Limit analysis and soil plasticity. Amsterdam (The Netherlands): Elsevier Science.
- Chen Z, Wang X, Haberfield C, et al. (2001) A three-dimensional slope stability analysis method using the upper bound theorem: Part I: theory and methods. International Journal of Rock Mechanics and Mining Sciences 38(3): 369-378. DOI: [10.1016/S1365-1609\(01\)00012-0](https://doi.org/10.1016/S1365-1609(01)00012-0)
- Dong J (2009) Study on three-dimensional soil arching effect of cantilever piles and ground resisting force acted on its build-in zone. Ph.D Dissertation, Chongqing University, Chongqing, China. (In Chinese)
- Dong J, Zhang YX, Wu SG, et al. (2009) Study of stability of soil



- between adjacent cantilever piles in incised slope. *Rock and Soil Mechanics* 30(12):3881-3888. DOI:10.16285/j.rsm.2009.12.054
- Gao YF, Zhang F, Lei GH, et al. (2012) An extended limit analysis of three-dimensional slope stability. *Geotechnique* 63(6): 518-524. DOI: 10.1680/geot.12.t.004
- Han C, Chen J, Xia X, et al. (2014) Three-dimensional stability analysis of anisotropic and non-homogeneous slopes using limit analysis. *Journal of Central South University* 21: 1142-1147. DOI: 10.1007/s11771-014-2047-8
- Macnab A (2002) *Earth retention systems handbook*. McGraw-Hill Professional Publishing
- Michalowski RL, Drescher A (2009) Three-dimensional stability of slopes and excavations. *Geotechnique* 59(10): 839-850. DOI: 10.1680/geot.8.P.136
- Paik KH, Salgado R (2003) Estimation of active earth pressure against rigid retaining walls considering arching effects. *Geotechnique* 53(7): 643-653. DOI: 10.1680/geot.2003.53.7.643
- Perko HA, Boulden JJ (2008) Lateral Earth Pressure on Lagging in Soldier Pile Wall Systems. *DFI Journal: The Journal of the Deep Foundations Institute* 2(1): 52-60. DOI: 10.1179/dfi.2008.006
- Shukla SK, Gupta SK, Sivakugan N (2009) Active earth pressure on retaining wall for c- $\phi$  soil backfill under seismic loading condition. *Journal of Geotechnical and Geoenvironmental Engineering* 135(5): 690-696.
- Skrabl S, Macuh B (2005) Upper-bound solutions of three-dimensional passive earth pressures. *Canadian geotechnical Journal* 42(5): 1449-1460. DOI: 10.1139/t05-067
- Soubra AH, Macuh B (2015) Active and passive earth pressure coefficients by a kinematical approach. *Proceedings of the Institution of Civil Engineers - Geotechnical Engineering* 155(2): 119-131. DOI: 10.1680/geng.2002.155.2.119
- Terzaghi K (1943) *Theoretical soil mechanics*. New York: John Wiley & Son.
- Vermeer PA, Punlor A, Ruse N (2001) Arching effects behind a soldier pile wall. *Computers and Geotechnics* 28(6): 379-396. DOI: 10.1016/S0266-352X(01)00010-6
- Wang YZ (2000) Distribution of earth pressure on a retaining wall. *Geotechnique* 50(1): 83-88. DOI: 10.1680/geot.2000.50.1.83
- Yang XL (2007) Upper bound limit analysis of active earth pressure with different fracture surface and nonlinear yield criterion. *Theoretical and Applied Fracture Mechanics* 47(1): 46-56. DOI:10.1016/j.tafmec.2006.10.003
- Zhang YX, Wang MM, Liu J, et al. (2014) Upper bound limit analysis of stability of soils between unbaffled cantilever anti-slide piles. *Chinese Journal of Geotechnical Engineering* 36(1): 118-125. DOI: 10.11779/CJGE201401010 (In Chinese)
- Zhou ML (2009) Study on the formation mechanism and influence factors of soil sliding shear band between unbaffled cantilever piles. Master Dissertation, Chongqing University, Chongqing, China. (In Chinese)